


Observation of enhanced thermal emission from patterned hyperbolic metamaterials

D. B. Fullager¹  · R. S. Hegde² · M. A. Fiddy¹

Received: 2 August 2015 / Accepted: 10 November 2015 / Published online: 31 March 2016
© Springer-Verlag Berlin Heidelberg 2016

Abstract Hyperbolic metamaterials (HMMs) are known to theoretically possess an unbounded range of wave vectors to which radiation can couple due to the hyperbolic shape of the HMM isofrequency surface. Thus, in practice, there exists a large range of modes that can be excited by thermal fluctuations that can then reradiate by coupling to high spatial frequency features. Herein, we show direct observation of enhanced thermal emission in an alternating gallium-doped zinc oxide (GZO) and zinc oxide (GZO/ZnO) multilayer HMM by utilizing a FLIR IR camera. This observation is supported by numerical simulations performed in CST MWS using index of refraction and extinction coefficient parameters obtained from an IR VASE.

1 Introduction

Recently, interest has grown in HMMs leading to new insights into the underlying physics governing subwavelength structures whose electromagnetic properties are well described by the effective medium approximation (EMA) [1]. The principal appeal of HMMs is that they do not rely on the use of narrow band resonances as did the initial realization of metamaterials (split ring resonators). HMMs

typically exhibit much broader ranges of operation and seem to hold more promise as a platform for truly engineering electromagnetic response in a material [2]. Currently, HMMs are divided into two types (I and II) whose namesakes are attributed to the number of negative components in their respective uniaxial permittivity tensors. Type I HMMs are cylinders or posts of a metal-like substance (negative permittivity) embedded in some positive permittivity structure. Type II HMMs consist of alternating layers of negative and positive permittivity materials such as alternating layers of metal and dielectric. It has been shown in the literature [3] that dielectric media offer more promise for low loss HMM device applications. As such, we focus on the use of doped/un-doped semiconductor layers for type II HMMs. Semiconductor-based HMMs are particularly appealing for use in the mid-IR range for applications that depend on modifying thermal radiation [4].

1.1 *K*-space dispersion of HMMs and EMT

The significant electromagnetic properties of HMMs can be easily visualized by using *k*-space isofrequency contours (IFCs). For the case of a uniaxial medium, which is sufficient for our purposes, the *k*-space IFC is determined by the permittivity tensor components.

$$\frac{k_x^2 + k_y^2}{\epsilon_z} + \frac{k_z^2}{\epsilon_{x=y}} = \frac{\omega^2}{c^2} \quad (1)$$

For the case of dielectrics, Eq. (1) leads to an ellipse in 3D space. In the event that we change the permittivity component parallel to the surface to normal, we then obtain a single-sheet hyperbola. The use of a single IFC to describe the *k*-space properties of a multi-component metamaterial has been well established as valid in the

✉ M. A. Fiddy
mafiddy@unc.edu

D. B. Fullager
dbfullager@gmail.com

¹ Department of Physics and Optical Science, University of North Carolina at Charlotte, Charlotte, NC, USA

² A*STAR Institute for High Performance Computing, Electronics and Photonics, Singapore, Singapore

literature [5] as long as the metamaterial is sufficiently well into the subwavelength regime. Once this condition is satisfied, we can safely invoke effective medium theory to determine the transverse permittivity component by averaging the permittivity components as a function of their fill fraction [6].

1.2 IFC dynamics

There are two cases of Eq. (1) which must be considered to understand how the IFC relates to the electromagnetic properties of the HMM in the effective medium regime. In the first case (Fig. 1 below), we see an effective permittivity greater than unity in the direction normal to the HMM's surface. In this case, the HMM is theoretically a perfect reflector as there are no modes which satisfy conservation of momentum transverse to the boundary which is a well-known requirement for propagation of electromagnetic waves.

The second case is shown in Fig. 2 below where the normal component of the permittivity is less than unity which creates an intersection between the IFC of the isotropic medium and the HMM. In this case, there are specific angles for each frequency that satisfy transverse momentum continuity at the boundary and allow for propagation. These regions are characterized by directional absorptivity or emissivity and enable novel applications that are reported elsewhere [7]. This condition is important to note because it demonstrates the importance of anisotropy of the constituent materials in generating interesting behavior in the HMM. If one extends this case to a normal permittivity component that is very near zero, the curvature of the hyperbola becomes extremely broad such that the IFC begins to resemble a cylinder. When this happens, a wave vector requires an enormous amount of momentum in the surface normal direction to satisfy the transverse continuity condition to radiate.

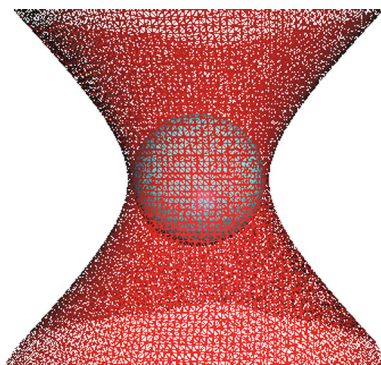


Fig. 1 HMM IFC compared to isotropic medium into which the HMM cannot radiate

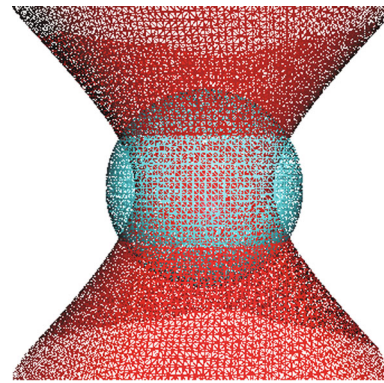


Fig. 2 HMM IFC shown intersecting with isotropic medium's IFC allowing for directional propagation into or out of the HMM

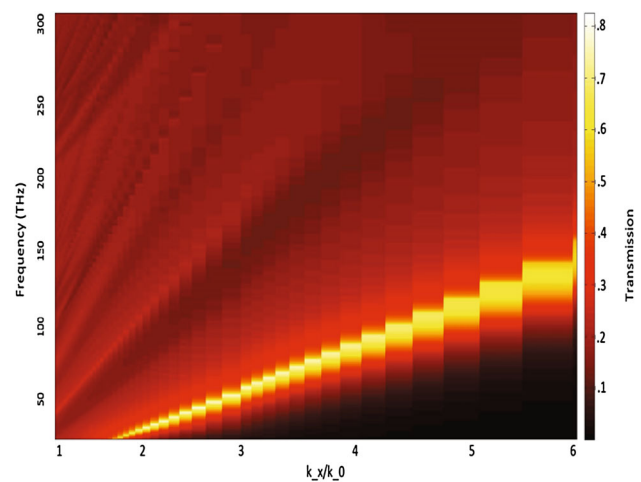


Fig. 3 Transmission as a function of the transverse wave vector to free space wave vector ratio and frequency

2 HMM fabrication and characterization

Herein, we provide brief details of the type II HMM fabrication as well as a reference to a more in depth analysis. Thereafter, we analyze the as-grown properties of the GZO/ZnO HMM (Fig. 3).

2.1 Fabrication details

A type II HMM was fabricated by means of molecular beam epitaxy (MBE) using electron beam evaporation of ultra-high-purity metallic zinc (99.99999 %) and RF oxygen plasma on c-plane sapphire (0.02° off m-plane). The substrate was thermally cleaned in ultra-high vacuum ($\sim 1\text{E} - 9$ torr) for 20 min at 800°C . The substrate temperature was then lowered to 600°C for growth of the HMM structure. Gallium flux was provided by a Knudsen cell at 950°C with the chamber's base pressure kept constant at $1\text{E} - 4$ torr. A Maxtek crystal thickness

oscillator was used to monitor the evaporated zinc flux, while the gallium flux was initiated and terminated at 100-nm thickness intervals eight times to create a 1.6- μm -thick HMM comprised of gallium-doped and (ideally) undoped ZnO. At the end of growth process, the HMM was annealed at 800 °C for 20 min. Detailed characterization has been provided elsewhere [8].

2.2 Dispersion simulation

Having obtained the index of refraction and extinction coefficients from a J. A. Woollam IR VASE, we turn our attention toward simulating the transmission through sub-wavelength gratings coupled to the fabricated HMM using CST μ -Wave Studio. The intent is to show that there are regions in the electromagnetic wave frequency versus grating spatial frequency plot that exhibit high transmission, thus ideally enabling the out-coupling of high wave vector modes associated with states which would otherwise be non-radiative since normally radiative modes are limited by the conservation of momentum. The grating period was swept from 50 nm to 10 μm with a duty cycle kept constant at 50 %. For the purposes of simulation, PECs were used for the grating material; however, recent results using gold as a grating material show nearly identical behavior. The ratio of free space wave vector to grating wave vector is given below.

$$k_x = k_0 \pm \frac{2\pi n}{\Lambda} \quad (2)$$

where Λ is the spatial period of the grating and n is an integer.

2.3 Thermal image

The realized HMM structure was then affixed to a Peltier heating setup using the same c -plane sapphire, and the HMM was grown on as a background to transfer heat from the Peltier heater to the HMM. In this manner, any ambiguity as to the contribution of the substrate can be addressed (Fig. 4).

A temperature contrast between the HMM and its background can clearly be observed. It is believed that this effect is a result of the HMM supporting more electromagnetic modes due to its higher photonic density of states (PDOS). Due to structural imperfections in the HMM which result from impurities, the lattice mismatch between ZnO and sapphire, and other miscellaneous factors mechanisms exist for high wave vector modes to couple into free space. While further study is required to be certain that the HMM is indeed out-coupling evanescent modes due to structural defects, it is worth noting that the sample which appears next to the HMM has the same composition but

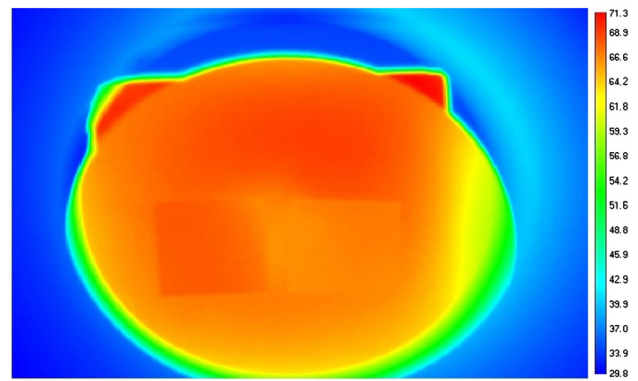


Fig. 4 FLIR IR image of the heated HMM sample (*small square on left*) next to a heated homogenized GZO/ZnO sample (*small square on right*) on top of a c -plane sapphire background heated by a Peltier heater

does not exhibit the hotter-than-background effect. An attempt was made to produce a 100-layer HMM of the same composition. However, due to the diffusivity of gallium in ZnO at high temperatures the resultant thin film is simply a gallium/zinc oxide ceramic. The absorptivity and emissivity of the imperfections believed to be responsible for evanescent out-coupling will be reported in a future work.

3 Discussion

From the measured physical properties of the fabricated HMM, it is clear that the HMM possesses the potential to support evanescent modes as propagating waves. The remaining challenge is to create an impedance match between the HMM and subwavelength features or otherwise pattern the HMM so that the normally non-radiative modes are allowed to propagate out of the HMM. We believe that we have shown evidence that naturally occurring defects can partially satisfy this role and plan to verify an enhancement in the power spectral density of the HMM's emission over that of a perfect black body in the part of the electromagnetic spectrum where the multilayer stack functions as a HMM.

4 Conclusions

We have shown that multilayer thin film HMMs can be fabricated in order to enable thermal emission exceeding that of the constituent materials from which they are made. We conclude that this apparent enhancement in thermal emission is a direct result of the sub-unity index in the HMM which we have previously reported [8] as well as surface roughness between the multiple layers which

enhances scattering of modes which are normally non-radiative.

Acknowledgments The authors are grateful for NSF support through the IUCRC International Innovation Fellowship awarded through the Center for Metamaterials and NSF Center for Metamaterials, Award Number 1068050.

References

1. Y. Guo et al., Applications of hyperbolic metamaterial substrates. *Adv. OptoElectron.* (2012)
2. Z. Jacob et al., Engineering photonic density of states using metamaterials. *Appl. Phys. B* **100**(1), 215–218 (2010)
3. A. Boltasseva, H.A. Atwater, Low-loss plasmonic metamaterials. *Science* **331**, 290–291 (2011)
4. C.L. Cortes, Z. Jacob, Photonic analog of a van Hove singularity in metamaterials. *Phys. Rev. B* **88**(4), 045407 (2013)
5. V.M. Agranovich, V.E. Kravtsov, Notes on crystal optics of superlattices. *Solid State Commun.* **55**(1), 85–90 (1985)
6. A. Poddubny et al., Hyperbolic metamaterials. *Nat. Photon.* **7**(12), 948–957 (2013)
7. I.S. Nefedov, L.A. Melnikov, Super-Planckian far-zone thermal emission from asymmetric hyperbolic metamaterials. *Appl. Phys. Lett.* **105**(16), 161902 (2014)
8. D. Fullager et al., Epitaxial thin films for hyperbolic metamaterials. in *SPIE OPTO*. International Society for Optics and Photonics (2014)